Research on Engineering Structures & Materials
www.jresm.org

Research Article

Structural performance of carbon-FRCM in strengthening and repairing pre-damaged RC slabs

Ali A. Abdulridha [*1,2,a], Majid M.A. Kadhima [1,b]

[1]*Department of Civil Engineering, University of Babylon, Hilla, Iraq*
[2]*Department of Civil Engineering, University of Warith Al-anbiya'a, Karbala, Iraq*

Article Info

Article History:

Received 14 Mar 2026

Accepted 16 May 2026

Keywords:

Carbon FRCM;
Structural repair;
Flexural strengthening;
Capacity restoration;
Cementitious matrix;
RC slabs

Abstract

This experimental study aims to investigate the structural behavior of a Carbon Fiber Reinforced Cementitious Matrix (C-FRCM) strengthening and repairing system. The experimental program was designed to assess two strengthening coverage levels: a full-surface coverage (100%) and a patch layout (50%) to evaluate the influence of material distribution. In order to assess the repair/strengthening efficiency, specimens were initially pre-loaded to 50% (in terms of applied force) of the ultimate load to introduce a controlled level of structural damage before the application of the FRCM system. The findings indicate that the Carbon-FRCM system can effectively improve the load-carrying capacity of undamaged slabs and contribute to the structural performance recovery of pre-damaged slabs under the investigated experimental conditions. All strengthened specimens exhibited load capacities higher than that of the control slab, suggesting the potential of the system as a strengthening and repair technique. The results also show that while full coverage provides higher stiffness and more uniform crack control, localized reinforcement can achieve significant improvement in load capacity with reduced material usage. Within the scope of the present experimental investigation, the Carbon-FRCM system exhibited promising structural performance as a strengthening and repair technique for reinforced concrete slabs under the investigated loading conditions.

1. Introduction

The growing degradation of reinforced concrete (RC) infrastructure is one of the major worldwide threats to the sustainability and resilience of our structured development [1, 2]. The combination of a few important factors, such as the development of corrosion due to material aging and aggressive environmental conditions (e.g., chloride ingress and carbonation), and increasing requirements imposed by new types of use that go beyond the original performance criteria lead to this structural degradation [3, 4]. The inadequacy of elements within the structural hierarchy are especially harmful to RC slabs, as they represent the most significant horizontal elements in the load-carrying system [5]. As a result, slabs are often among the most critical structural components in terms of serviceability, as they are highly susceptible to excessive deflection and flexural cracking, which may adversely affect the overall structural performance of the building system [6]. Nevertheless, the need for intervention for slab systems can be categorized into two engineering challenges: proactive "strengthening" for higher loading protocols and reactive "repairing" to recover structural capacity lost due to damage or environmental degradation. In either context, the ultimate goal is to extend the service life of existing structures while reducing the environmental and economic costs of complete demolition and reconstruction [7]. In retrospect, this led to a shift away from cumbersome traditional practices such as steel plate bonding, characterized by

*Corresponding author: eng957.ali.abadulrazzaq@student.uobabylon.edu.iq
[a]orcid.org/ 0009-0005-4908-3737; [b]orcid.org/0000-0003-2464-0048
DOI: http://dx.doi.org/10.17515/resm2026-1568st0314rs

corrosion vulnerability and installation related difficulties, to use of expensive composite materials in structural retrofitting [8].

The later introduction of Fiber Reinforced Polymer (FRP) composites marked a revolution in structural rehabilitation. With outstanding strength-to-weight ratios and natural resistance to corrosion, FRP systems made with carbon, glass or aramid fibers encapsulated in organic epoxy resins provided an efficient solution for flexural and shear capacity increases with minimal changes in structural geometry [9-11]. However, there are very considerable technical limitations associated with FRP because of the approach used they are dependent on organic polymers which persist in the environment. In particular, epoxy resins exhibit poor thermal properties which may result in loss of bond integrity and catastrophic failure during fire conditions. In addition, the impervious quality of FRP creates a vapor barrier, which can keep moisture inside the concrete that can lead over time to delamination, or freeze-thaw damage [12]. In order to avoid these thermal and chemical incompatibilities, Fiber Reinforced Cementitious Matrix (FRCM) has been proposed as a more compatible and "breathable" reinforcement alternative [13].

Due to the use of an inorganic, mineral-based cementitious mortar instead of organic epoxy, FRCM provides excellent fire resistance and avoids a potentially detrimental chemical interaction with the concrete substrate [14, 15]. Symmetrically, FRCM provides a complex bond-slip mechanism as well as a multi-linear stress-strain response that fosters a more ductile failure mode in comparison to the brittle debonding of FRP applications [16, 17]. When the cementitious matrix experiences micro-cracking at a threshold level, the crack will become consolidated so that the load is progressively redistributed across the fiber mesh, resulting in an amount of strain warning that is dispersed as diffuse micro-cracking rather than catastrophic failure [18]. While FRCM is already established as an effective technique to strengthen undamaged load bearing members, the "repair" of structurally damaged elements presents new engineering challenges [19]. It also requires the repair of already greatly sustained damage members which requires a method of fusing macro-cracks existing while also being able to restore sectional stiffness. Here the reinforcement coverage ratio is a key ballpark figure for performance as well as cost performance. One approach is to use localized patches (or sheets) instead of the full-surface coverage, this is a strategy to reduce material consumption especially because carbon fiber is very expensive, without sacrificing the total capacity uptake [20].

Recent life-cycle cost analyses also corroborate this paradigm shift, indicating that although FRCM entails more labor at the outset, the increased durability with decreased long-term maintenance requirements makes it a relatively more economical solution through the life of a structure [19, 21, 22]. Therefore, the current research aims to study the behavior of reinforced concrete slabs strengthened with Carbon-FRCM under loading with two possible strengthening ratios: full surface coverage and localized application in the region of maximum moment. In particular, the capacity of partial strengthening configurations to produce efficient stress redistribution and crack control with limited materials is emphasized in this work. Furthermore, the main aim of this study is to evaluate the structural performance recovery of slabs pre-damaged at moderate damage levels (50% of the ultimate load of the control specimen) and subsequently repaired using Carbon-FRCM. The paper presents a detailed investigation on load–deflection behavior, stiffness development and failure modes to increase the understanding of the interaction of the structural behavior between the cementitious matrix, textile reinforcement and the damaged concrete substrate in two-way slab systems.

2. Experimental Program

2.1. Materials

2.1.1 Cementitious Mortar

In fiber- reinforced cementitious matrix (FRCM) composite, the cementitious mortar serves as the inorganic binding matrix that encapsulate the textile reinforcement and facilitate stress transfer between the reinforcement and the concrete substrate [23, 24]. An appropriate cementitious matrix is critical for load redistribution, bond performance and long-term durability in strengthening members [25]. For the present study, the cementitious mortar selected was Sika MonoTop®-612[26], a one-component, fiber-reinforced, polymer-modified structural repair mortar that meets the requirements of Class R3 according to EN 1504-3[27]. According to the product's technical specification, the mortar comprises of cement, specified aggregates, silica fume, polyamide fibers, and additives, and appears as a gray powder that is mixed with clean water prior to application. The mortar was made carefully according to the manufacturer's specifications, assuring a constant water-to-powder ratio, complete mixing (mechanical mixer at low speed), and proper handling to produce uniform workability. The mechanical properties and technical specification of the mortar, obtained from the manufacturers data sheet are listed in Table 1. It should be noted that the material properties reported in this study are based on manufacturer technical data sheets for commercially available FRCM components, and no additional experimental characterization of the composite system or interface behavior was performed within the scope of this study.

Table 1. Properties of Sika MonoTop®-612

Property	Description
Composition	Polymer-containing cementitious mortar with different additives and synthetic fiber.
Appearance / Colour	Grey powder
Maximum grain size	Dmax: 2.0 mm
Compressive strength	28 days (ASTM C109) ~40 MPa *Testing cubes 50 x 50 x 50 mm
Mixing ratio	3 - 3.25 L of water per 25 kg bag
Fresh mortar density	Fresh mortar density 1.95 kg/L at +20 °C
Layer thickness	Min. 5 mm, Max. 30 mm

2.1.2 Fabric-Reinforced Cementitious Matrix (FRCM) Textile

In fabric-reinforced cementitious matrix (FRCM) systems, textile reinforcement represents the main load-carrying component responsible for controlling the tensile response and governing the overall structural performance of strengthened members [17, 19]. Textile reinforcement in FRCM has a high tensile capacity and durability better than FRP under severe environmental and thermal conditions due to its inorganic matrix and better compatibility with concrete [28]. Carbon, glass, basalt, and polyparaphenylene benzobisoxazole (PBO) fibers have all been used in FRCM applications, with each having its own mechanical and durability properties [19].

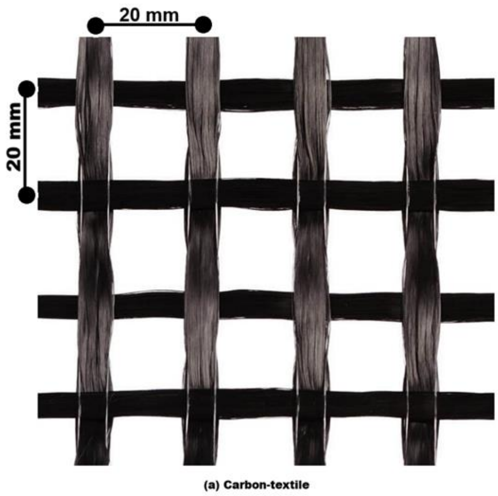

Fig. 1. Selected carbon-textile

Textile reinforcements are chosen based on their performance and durability for application within FRCM systems. Carbon fabrics are characterized by impressive high tensile strength, high elastic modulus, low creep, and long-term stability [19, 28, 29], which are favorable for high-performance strengthening applications. In this study, carbon textile was used as reinforcements in the FRCM system and the mechanical behavior was compared under flexural loading. The carbon textile has composite nominal thickness of 0.047 mm and mesh size of 20 × 20 mm as shown in Fig. 1. Table 2 summarizes the mechanical properties of the textile while Fig.1 shows its nature within the strengthening system.

Table 2. Characteristics of FRCM textile based on the manufacturer's data sheet.

Material	Nominal thickness	Tensile strength	Modulus of elasticity
Carbon	0.047 mm	3600 MPa	230 GPa

2.1.3 Reinforced Concrete

2.1.3.1 Reinforcing Steel

Reinforcing steel improves reinforced concrete by providing tensile strength, ductility, and greater bond with concrete, minimizing cracking and enhancing structural load-bearing capacity [29]. 6 mm diameter deformed bars were used in the present work to provide better interlocking of mortar and bond strength. All reinforcing bars shall conform to the ASTM A615/A615M-20 [30] standard specification for deformed and plain carbon-steel bars for concrete reinforcement, providing consistent chemical and mechanical properties. Calibrated micrometers were used to take measurements for the diameter and thickness of the bars; tensile testing was performed according to ASTM standards to determine yield and ultimate strength for the selected Grade 40 steel (ASTM A615/A615M-20) [30]. A detailed mechanical property of the reinforcing steel can be found in Table 3.

Table 3. Properties of reinforcement steel

Property	values
Nominal diameter (mm)	6
Actual diameter (mm)	5.8
Cross-sectional area (mm^2)	26.4
Yield stress (MPa)	405.3
Ultimate stress (MPa)	605
Elongation (%)	17
Nominal weight (Kg/m)	0.208
Grade	G40

2.1.3.2 Concrete

Concrete is one of the most widely used construction materials due to its high compressive strength, good durability and it can be applied in various structural applications [31]. The mechanical properties of the normal-strength concrete oriented in this study were evaluated using the standard tests compressive strength, splitting tensile strength and flexural strength to give an overview of its structural behavior. Compressive tests were performed on standard cubes measuring 100mm × 100mm × 100mm, while standard cylindrical 100mm × 200mm test pieces were employed for tensile tests, and the flexural strength of the prism specimens was determined. All tests were conducted according to British Standards BS 1881 with the customs loading rates. Table 4 will illustrate the concrete standards and the measured values.

Table 4. Summary of concrete mechanical properties

Property	Specimen Type	Average (MPa)	Test Standard
Compressive Strength	Cube	34.8	BS 1881: Part 116 [32]
Splitting Tensile Strength	Cylinder	2.27	BS 1881: Part 117 [33]
Flexural Strength	Prism	5.58	BS 1881: Part 118 [34]
Modulus of Elasticity	N/A	27.7 GPa	Empirical formula

2.2 Test Specimens and Parameters

2.2.1 Overview

An experimental program was developed to study the flexural performance, strengthening effectiveness, and general behavior of Fabric-Reinforced Cementitious Matrix (FRCM) strengthened reinforced concrete (RC) slabs. In order to have similar boundary conditions and also general characteristics from the test specimens, a total of five square RC slab specimens were fabricated having identical geometry, thickness, and boundary conditions. The specimens were constructed of 1.0 m × 1.0 m plan dimensions to correspond to a representative plan size of scaled RC slabs and accommodating laboratory constraints.

2.2.2 Geometry and Reinforcement

The reinforced concrete slab specimens were all 1.0 m × 1.0 m in plan and had a consistent thickness of 80 mm. The concrete cover was kept 15mm for all the reinforcement. All specimens had the same geometry and reinforcement layout. There were two orthogonal directions of main flexural reinforcement spaced at 192 mm with 6 mm diameter steel bars. The main reinforcement was arranged accordingly so that the slab bottom face received the reinforcement on both the total area of slab perimeter. The bottom rebar at the slab edges were bent up at 180° at the supports in order to give them continuity at the slab perimeter, which formed the top rebar. Next to the supports, localized top reinforcement was provided with bent bars, which were oriented perpendicular to each edge and spaced at 192 mm.

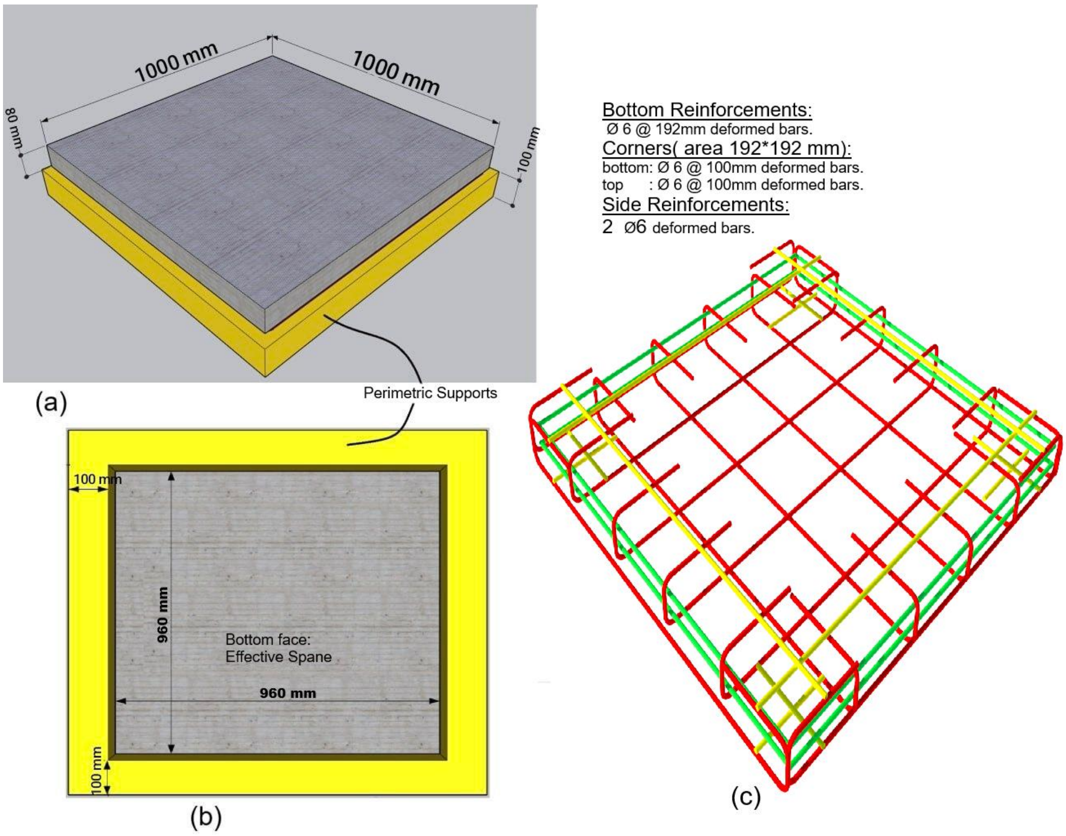

Fig. 2. (a) The slab's geometry; (b) the slab's perimeter-supported bottom face; and (c) the slab's steel reinforcement details

Reinforcement detailing has been further improved to enhance anchorage behavior and crack control, and to mitigate stress concentrations near the slab edges and corners. By addition, two further 6 mm bars were placed at the bottom face of the slab within a square area of 192 mm × 192 mm at each corner of the slab, leading to an effective reinforcement spacing of around 100 mm in this area. In addition, on the top face, a 6 mm bar was placed parallel to the edges of each slab, 100 mm from the edge, with a length of 960 mm. Due to having these edge bars, the density of reinforcement at corners of slab on its top face were increased with a spacing of 100 mm (approx). The above-mentioned details led to better anchorage behavior, better bond and crack distribution as well as lower stress concentration in these critical areas. Fig. 2(a), (b) and (c) shows the slab geometry, bottom face of perimeter supported slab, and the reinforcement layout respectively.

2.2.3 Studied Parameters

This experimental program was developed to study the effect of strengthening material, strengthening configuration, and preloading condition on the flexural behavior of two-way reinforced concrete slabs. For reliable comparison, all other parameters such as concrete characteristics, slab dimensions, reinforcement ratio, mortar type, loading conditions, support conditions, and effective span were kept constant in this experimental program.

The parameters ranged as ratio of strengthened area to effective span, and loading condition (unloaded or 50% pre-loaded to the ultimate load of the control slab during FRCM strengthening). Therefore, one specimen was tested without the strengthening as a control slab and indicated with an R.

The strengthening schemes included slabs strengthened before loading with various fiber reinforced cementitious matrix (FRCM) configurations of carbon fiber, including continuous strengthening with two layers covering 100% of the effective bottom surface (C2100), as well as two orthogonal layers covering 50% of the effective span applied as continuous layers in the max moment region (C250). Also prior to strengthening, two slabs were preloaded to 50% of the control slab capacity to mimic conditions of retrofitting, denoted as CD250 and CD2100, respectively. Fig. 3 provides a schematic illustration of the strengthening configurations, and Table 4 summarizes the specimen details and test variables.

2.2.4 Specimen Notation

The notations used to designate each tested specimen according to its strengthening condition and configuration are presented schematically in Table 4, where R is the reference specimen tested without any strengthening and that serves as the control slab. Specimen C250 is a completely unloaded slab that has been reinforced with a carbon-based FRCM system. Here, two orthogonal carbon textile layers were layered in the region of Mmax, both covering 50% of the effective span in a continuous way. Two Continuous carbon FRCM layers fully covering the effective bottom surface were used as the strengthening solution for specimenC2100.

Table 4. Samples, experimental parameters, and materials

Specimen	Strengthening Material	Number of Layers	Strengthening Layout	Coverage (% of effective span)	Preload Condition	Notes
R	None	None	None	None	None	Control slab
C250	Carbon	2	Continuous sheets	50	None	Applied in maximum moment zone
C2100	Carbon	2	Continuous	100	None	Full bottom surface coverage
CD250	Carbon	2	Continuous sheets	50	Preloaded 50%	Retrofitting condition, Applied in maximum moment zone
CD2100	Carbon	2	Continuous	100	Preloaded 50%	Retrofitting condition, Full bottom surface coverage

To evaluate retrofitting scenarios, specimens CD250 and CD2100 were initially preloaded to 50% of the control slab's ultimate capacity prior to strengthening. Specimen CD250, identical in configuration to C250, was reinforced with two orthogonal carbon Fiber-Reinforced Cementitious

Matrix (FRCM) layers covering 50% of the effective span. Similarly, specimen CD2100, mirroring specimen C2100, was strengthened with two continuous carbon FRCM layers integrated along the entire bottom effective surface.

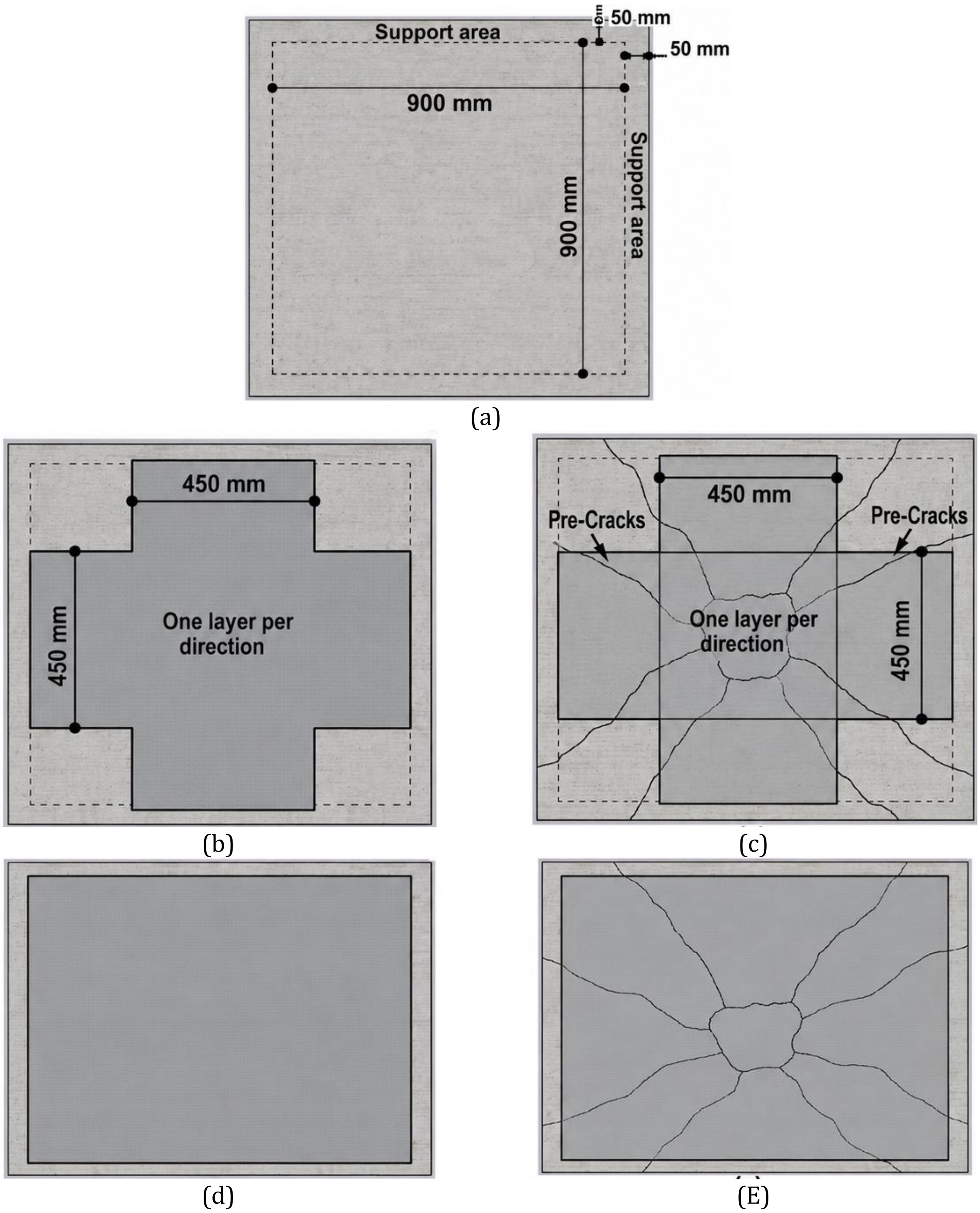

Fig. 3. Configuration of FRCM strengthening on the tested samples/ (a) Control slab R, (b) C250, (c) CD250, (d) C2100 (e) CD2100

2.3 Retrofitting Procedure

The systems used to strengthen and retrofit the reinforced concrete slab specimens in this experimental program included the use of fabric-reinforced cementitious matrix (FRCM) systems with carbon textile, which are known to have high tensile properties, good durability, and compatibility with cement-based substrates ([19, 36]. All specimens followed the same consistent and reproducible strengthening procedure, which is schematically depicted in Fig. 4. Before the strengthening, the tension faces of the concrete were mechanically cleaned to get rid of dust, laitance, and loose materials. A shallow grid of grooves (about 2 mm in depth) was implemented on the concrete surface to increase the bond effectiveness and the mechanical interlock between the substrate and the cementitious matrix (Fig. 4a).

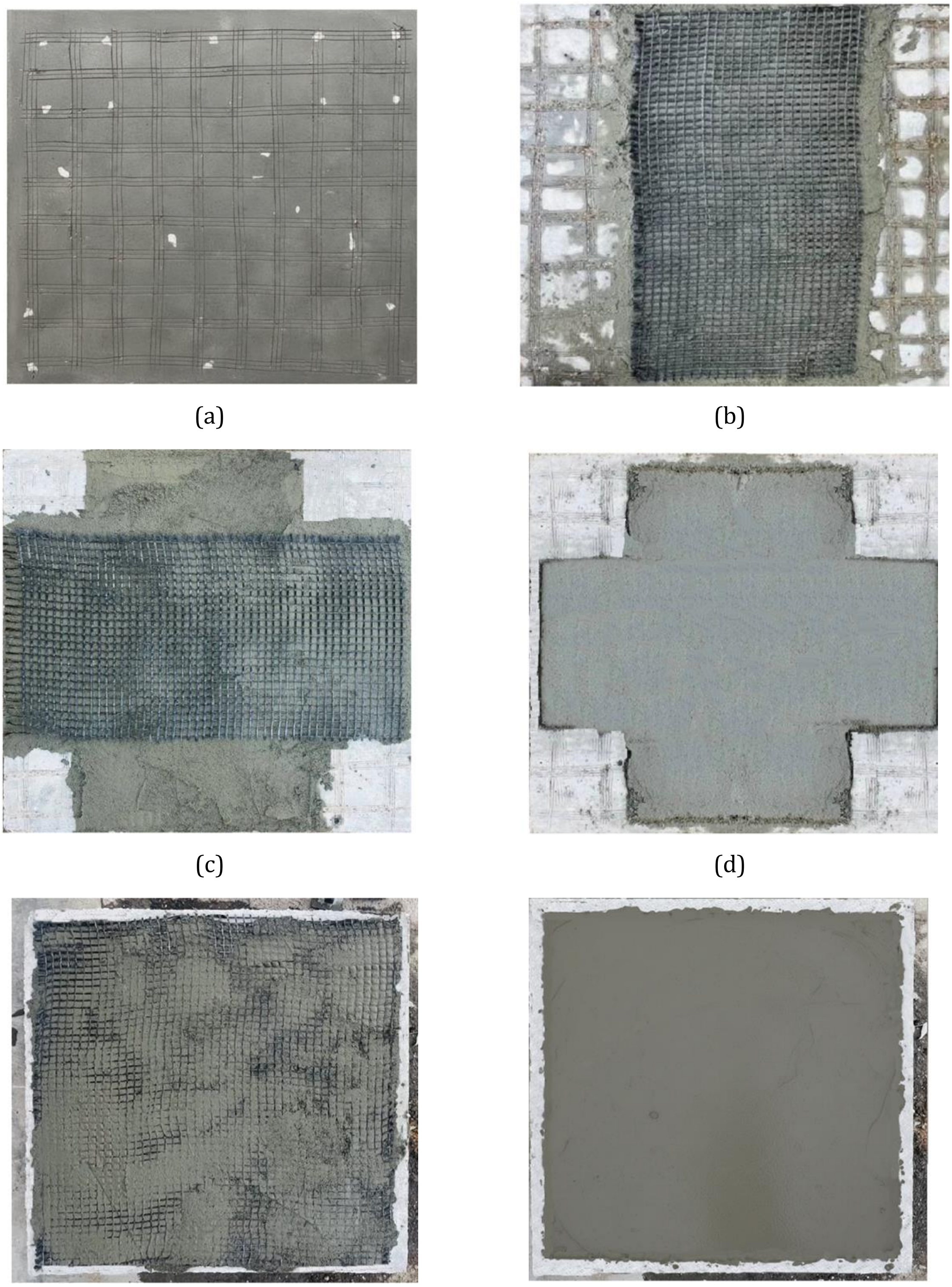

(a) (b) (c) (d) (e) (f)

Fig. 4. Application steps for FRCM reinforcement: (a) Preparing and Moistening the concrete surface for strengthening; (b and e) Application of the first mortar layer together with the carbon textile; (c) Application of the second mortar layer along with the carbon; (d and f) Application and finishing of the final mortar layer

Moistening of the prepared surfaces was performed to improve adhesion before mortar application. Then, a first layer of cement-based mortar (approximately 3 mm thickness on average) was applied on the area where the strengthening would be performed, according to the strengthening layout given by the notation of the specimens. The carbon textile reinforcement for each specimen was specifically prepared and cut in accordance with the designated strengthening configuration. The textile was embedded and lightly compacted by hand, while the mortar was still fresh, to guarantee proper contact and impregnation as well as avoid air voids (Fig. 4b and e).

More layers of mortar were applied to fully encapsulate the textile, followed by the placement of another layer of textile (Fig. 4c). This successive layer was applied with sufficient care for to settle correctly and bond. The strengthening process concluded with the application of a final thin layer of mortar and meticulous finishing/smoothing of that surface, as seen in Fig. 4(d and f). Following strengthening, all the specimens were cured until the adequate mechanical performance of the FRCM system was achieved before proceeding with the tests. To facilitate evaluation and comparison of the effects FRCM system in both strengthening and repairing for the flexural behavior of the slabs, the same strengthening treatment was uniformly applied across all slabs.

2.4 Test Setup and Loading Protocol

The testing of all the slab specimens was done using a four-point loadin configuration with a universal testing machine of capacity 2000 kN. The four edges of the slabs are simply supported with a continuous support system along the slab perimeter. The support framework has 4 steel beams each welded to a steel bar 25 mm in diameter. In order to provide uniform stress transfer and avoid local stress concentrations each of the steel bars, prior to placement of the concrete slab, had a 10 mm wide rubber strip placed on the top face so that the slab tension face was in direct contact with the support system.

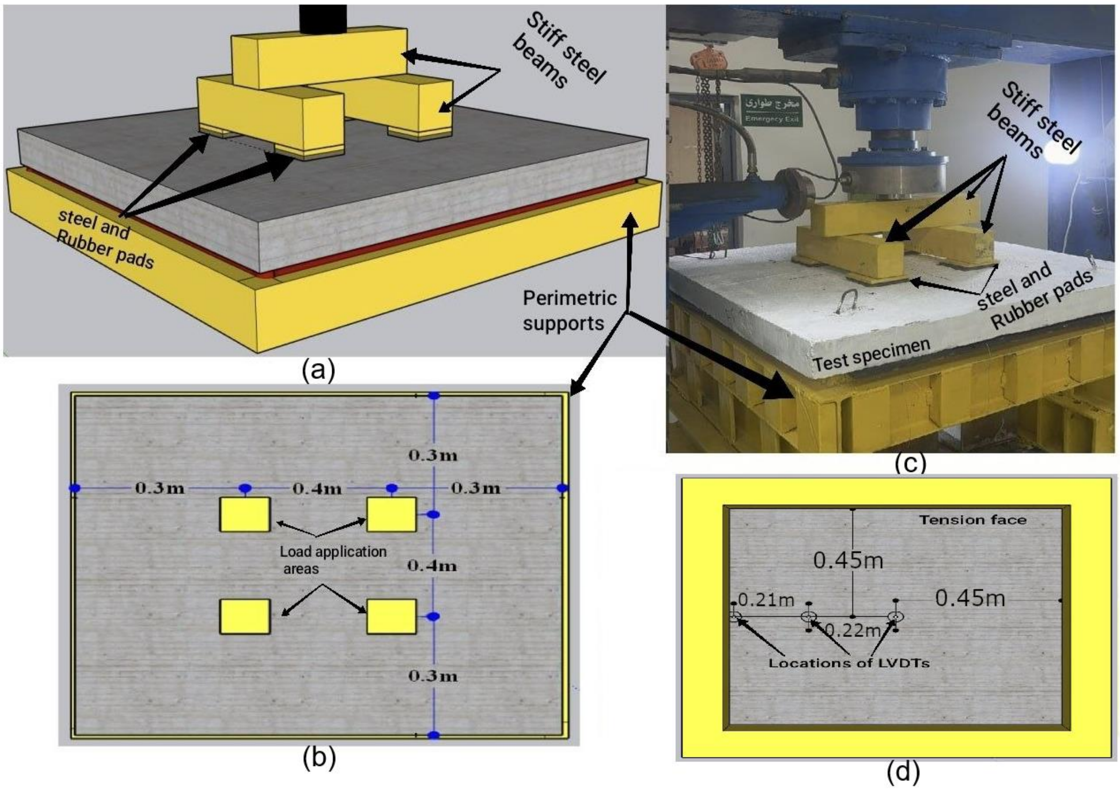

Fig. 5. Experimental setup (a) 3D schematic view; (b) top view; (c) the specimen positioning and the applied loading scheme; (d) Layout of LVDTs installed for deflection measurements

A four-point bending setup was used for the loading, as highlighted in Fig. 5(a and c) which applied the loading in a load-controlled manner. The applied load from the testing machine was initially transferred to the high-strength steel spreader beam and then to two transverse steel beams (one on each side of the primary beam) oriented perpendicular to the primary beam. Each transverse beam transmitted the load to the slab through two loading points at 300 mm from slab edges, leading to a distance of 400 mm between loading points centers. A square steel plate 100 x 100 mm comprising 12 mm thick was inserted between the steel beam and slab followed by a 100 × 100 × 10 mm rubber plate to reduce the local crushing of the concrete surface and allow uniform distribution of load at each loading location. All slabs retained an effective span of 960 mm.

In the test setup, the machine load cell recorded the applied load and three linear variable displacement transducers (LVDTs) were used to obtain slab deflections as shown in Fig. 5 (d). In the geometry, one LVDT was placed at the center of the slab where the maximum mid-span deflection would occur, and the other two were placed between the support and the center of the slab, one close to the support, to enable direct comparison of deflection measurements. Visual inspection for monitoring crack initiation, propagation, and failure patterns was conducted periodically during the tests, and crack widths were examined using a crack width gauge. However, these observations were used primarily for qualitative interpretation of crack development and failure behavior, and were not systematically recorded for a quantitative serviceability assessment based on crack-width criteria. All specimens were monotonically loaded to failure. For the retrofitted specimens (CD250 and CD2100), a pre-loading was applied up to 50% of the ultimate load of Specimen R, then followed by unloading, strengthening, and subsequent reloading until failure. The same test setup, instrumentation, and loading protocol were employed for all specimens to ensure uniformity and facilitate comparative evaluation of the flexural behavior and strengthening efficiency of the various test configurations.

3. Results and Discussion

In this section, the results related to flexural performance of the tested RC slabs are discussed in detail. It serves as an experimental study aiming at understanding the structural performance, load-carrying capacity and deformation behavior of the specimens. Particular attention is given to the serviceability behavior of the slabs in terms of stiffness development and deflection response, with reference to the general principles of the short-term serviceability limit state (SLS) described in Eurocode 2—Part 1 (CEN 2004). In the present study, the serviceability load level (PSLS) was determined based on the deflection limit equal to l/250, where l represents the effective span of the slab. For the tested specimens, this deflection corresponds to 3.6 mm, and the associated load values were obtained directly from the experimental load–deflection curves. This approach enables a comparative interpretation of slab behavior and identification of the load range corresponding to deflection-based serviceability performance within the scope of the present experimental study. In addition, the stiffness (k) of the slabs was evaluated quantitatively at various loading stages (both pre-cracking and post-cracking). Stiffness was determined from the slope of the load–deflection curves, where the initial stiffness (k_i) corresponds to the approximately linear portion of the response before first cracking, and the post-cracking stiffness (k_p) represents the response after crack initiation and before the final nonlinear softening stage, as defined by the following equation.

$$k = \Delta P \,/\, \Delta\delta \qquad (1)$$

Where P represents the applied load and δ denotes the corresponding mid-span deflection.

In order to ensure a clear and structured comparison, each subsequent subsection contains:

- A table compilation providing the context of the primary mechanical characteristics and markers of functionality.
- Load-deflection curves to demonstrate the general trends in behavior.
- Photo Record of Failure Modes to see the crack patterns and failure modes of each specimen at ultimate state.

3.1 Strengthening Efficiency of FRCM System

The experimental observations summarized in Table 5 indicate the beneficial influence of the Carbon-FRCM system on the structural response of the tested slabs. The first crack load (Pcr) of both specimens C250 and C2100 was identical at 40 kN which corresponds to 166.7% higher than standard control slab (R). These results suggest that partial coverage (C250) can provide crack-delay behavior comparable to that of full coverage (C2100) under the investigated loading conditions. For the ultimate bearing capacity (Pu), as shown in the Load-Deflection diagram (Fig.

6), C 2100 recorded 163 kN compared to 153 kN for C250. Despite using approximately 50% less carbon textile reinforcement, specimen C250 achieved approximately 93.8% of the ultimate load capacity recorded for specimen C2100.

The experimental response indicates that the strengthening configuration significantly influenced the stiffness development and post-cracking deformation behavior of the tested slabs. The first stiffness (ki) of specimen C250 appeared to be 17.05 kN/mm, a significant increase over that of the reference slab (10.6 kN/mm), and the maximum for the C2100 specimen was 25 kN/mm. A similar trend was observed for the post-cracking stiffness response (k_p), reflecting the influence of the strengthening configuration on stiffness retention after crack initiation, with C2100 (4.6 kN/mm) performing better than C250 (3 kN/mm). For serviceability, based on Eurocode 2 requirements, C250 improved the service load (PSLS) to 55 kN (77% improvement over R) and C2100 to 70 kN.

From a material efficiency perspective, specimen C250 may represent a practical strengthening option, as comparable structural improvement was achieved using a reduced amount of carbon textile. It should be noted that no detailed economic analysis was performed in this study, and the comparison is limited to relative material usage between strengthening configurations. The ultimate load for C250 was 6.5% lower than that of C2100; However, the doubling of the reinforcement area in C2100 did not result in a proportional increase in structural performance, as reflected in the corresponding deflection values (11.93 mm for C2100 compared to 15.55 mm for C250). While full-surface strengthening (C2100) provides modest gains in capacity and stiffness, the results indicate that localized strengthening (C250) can achieve efficient structural performance with reduced material usage, making it a practical option for engineering applications.

Table 5. Summary of experimental results for specimens: R, C2100, and C250

Specimen ID Configuration	R None	C2100 Continuous	C250 sheet
Layers	None	2	2
P_{cr} (kN)	15	40	40
P_u (kN)	120	163	153
Δ_u(mm)	21.34	11.93	15.55
P_{SLS}	31	70	55
k_i (kN/mm)	10.6	25	17.05
K_p(kN/mm)	1.13	4.6	3
Preloading level	None	None	None

Qualitative data from visual evidence of the failure modes in Fig. 7 supports these numerical data. The control slab (R) experienced wide, localized flexural cracks. In contrast, failure of the strengthened specimens showed the "multi-cracking" mode. Localized stress-bridging was observed in cracks concentrated within and along the edges of the reinforced patch in C250. In contrast C2100 showed its tension face filled with a densely distributed network of fine cracks (crack smearing). The extensive crack branching observed in specimen C2100 suggests that the continuous Carbon-FRCM configuration contributed to a more distributed transfer of tensile stresses across the tension zone. This behavior was associated with improved stiffness retention and lower deflection values prior to ultimate failure. The observed structural behavior can be further interpreted based on the interaction between the cementitious matrix, textile reinforcement, and cracked concrete. After the onset of cracking, the FRCM system contributes to tension stiffening by bridging flexural cracks and transferring tensile stresses across the cracked sections. In the localized configuration (C250), this mechanism is concentrated within the strengthened region, resulting in partial stress redistribution and localized crack control. In contrast, the continuous configuration (C2100) promotes a more uniform stress distribution over the entire tension zone, leading to improved stiffness retention and more distributed cracking patterns. This behavior may explain the enhanced stiffness retention and reduced deflection observed in the fully strengthened specimens under the investigated loading conditions. It should be noted that the presented results are based on a limited number of specimens and are intended to reflect observed behavioral trends under controlled laboratory conditions rather than generalized structural performance.

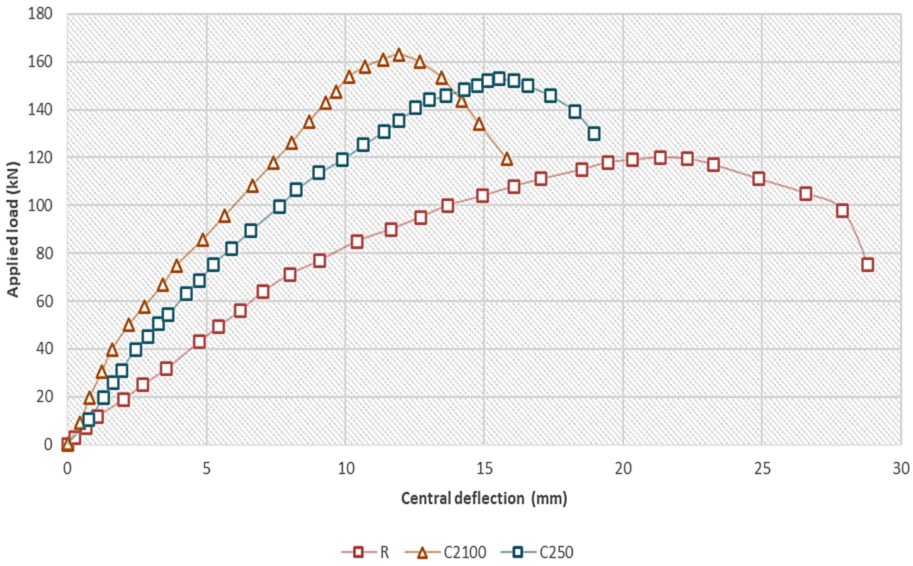

Fig. 6. Load-deflection response of specimens: R, C2100, and C250

(a) (b) (c)

Fig. 7. Failure modes and crack patterns of specimens: (a) R, (b) C250, and (c) C2100

3.2 Repair Efficiency of FRCM System

The functionality of the Carbon-FRCM system in rehabilitating and upgrading the pre-damaged RC slabs is discussed here. The specimens CD250 and CD2100 were pre-loaded with 60 kN, i.e. 50% of control slab (R) ultimate capacity. The purpose of this pre-loading phase was to induce controlled flexural cracking representative of a moderate pre-damage condition prior to strengthening, defined in this study based on the applied preload level rather than on quantitative damage indices. This approach allows a consistent comparison of the effectiveness of different strengthening configurations while maintaining the structural integrity of the specimens. It should be noted that the pre-damage condition was defined solely based on the applied preload level corresponding to 50% of the ultimate capacity of the control specimen. Although this loading stage produced visible flexural cracking representative of a moderate damage condition, no quantitative measurements of crack width, residual deflection, or stiffness degradation were systematically recorded prior to strengthening. Consequently, the initial damage state could not be characterized using quantitative damage indices. Therefore, the repair efficiency discussed in this study should be interpreted as a comparative structural response under a controlled preloading condition rather than as a fully quantified assessment of damage recovery. As shown in Table 6, all the experimental results indicated that the damaged slabs were successfully repaired to their original capacity or even greater than that using the FRCM system. In particular, specimen CD2100 attained an ultimate load of 156.5 kN whereas CD250 achieved 132.9 kN, which are greater than the undamaged control slab by 30.4% and 10.7% respectively.

The repaired specimens exhibited partial recovery of post-cracking stiffness following the application of the Carbon-FRCM system. The post-cracking stiffness (kp) evaluated increased dramatically; kp for specimen CD2100 was 3.5 kN/mm; kp for specimen CD250 was 1.6 kN/mm, both values much greater than the 1.13 kN/mm for the cracked control specimen. Although there were already cracks in the concrete, the load-deflection curves of Fig. 8 show a stable transition and good load transfer from the damaged concrete substrate to the carbon fiber mesh via the cementitious matrix. The observed failure mode was primarily characterized by rupture of the carbon textile without significant visible debonding of the FRCM layer. This behavior suggests that an effective stress transfer mechanism developed between the cementitious matrix and the concrete substrate under the investigated loading conditions. It should be emphasized that no direct bond-slip tests, interface strain measurements, or detailed interfacial characterization were conducted in the present study. Consequently, bond behavior is interpreted indirectly based on the observed structural response and failure patterns, and should be considered as an observational assessment rather than a direct experimental verification.

Table 6. Summary of experimental results for specimens: R, CD250, and CD2100

Specimen ID	R	CD250	CD2100
Configuration	None	sheet	Continuous
Layers	None	2	**2**
P_{cr} (kN)	15	None	None
P_u (kN)	120	132.9	156.5
Δ_u(mm)	21.34	14.2	14.5
P_{SLS}	31	None	None
k_i (kN/mm)	10.6	None	None
K_p(kN/mm)	1.13	1.6	3.5
Preloading level	None	50%	50%

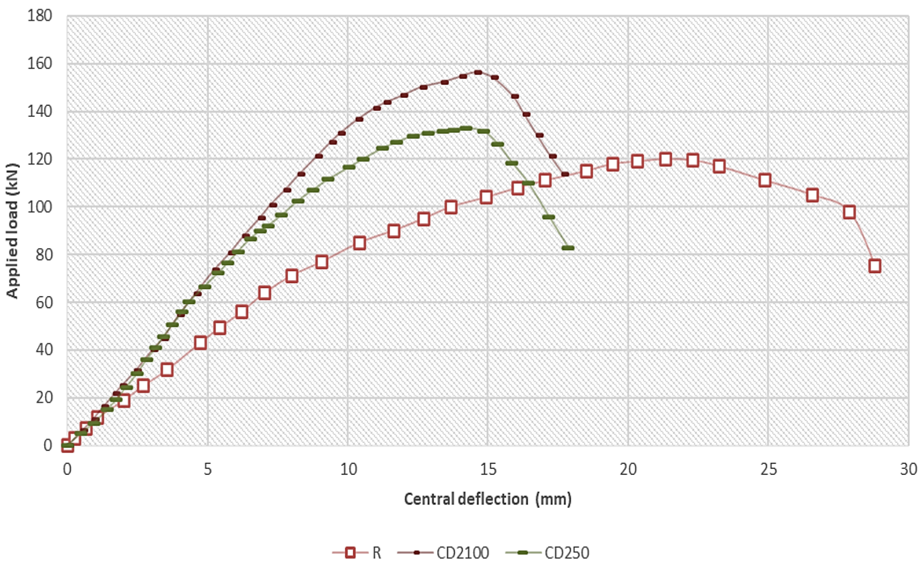

Fig. 8. Load-deflection response of specimens: R, CD2100, and CD250

From a structural performance perspective, the comparison between specimens CD2100 and CD250 provides useful insight into the influence of strengthening extent on slab behavior. Although the CD2100, with full surface coverage, demonstrated a 17.7% increase in ultimate load capacity compared to the localized configuration CD250, this improvement was associated with a significant increase in the amount of reinforcement used. This non-proportional relationship indicates that while the continuous configuration enhances capacity and stiffness, the increase in reinforcement quantity is significantly higher relative to the achieved performance gain. On the other hand, specimen CD250 achieved full recovery of the pre-damaged slab, delivering a 10.7% increase in load capacity compared to the control specimen while using a reduced amount of reinforcement relative to CD2100. This highlights the ability of localized strengthening to provide effective structural improvement with lower material usage. This observation is further supported by visual inspection of the crack patterns shown in Fig. 9. While CD2100 exhibited a more distributed crack pattern, the localized reinforcement in CD250 effectively controlled major flexural cracks and prevented premature failure. These results suggest that strategic placement of FRCM in critical tension zones can provide efficient structural enhancement without the need for full surface coverage.

(a) (b) (c)

Fig. 9. Failure modes and crack patterns of specimens: (a) R, (b) CD250, and (c) CD2100

3.3 Comparative Structural Performance of Carbon-FRCM: Strengthening vs. Repair

The experimental outcomes indicate that the Carbon-FRCM system can provide effective strengthening and repair performance for reinforced concrete slabs under the investigated conditions, since all the rehabilitated specimens reached an ultimate capacity higher than the control slab (R=120 kN), as indicated in Table 7. The comparison of the ultimate load capacities (P_u) indicates that the repaired specimens (CD series) achieved structural responses comparable to or greater than that of the control specimen under the investigated experimental conditions Specimen CD2100 reached an ultimate load of 156.5 kN, which is the equivalent of 96% of the strength capacity of its retrofitted equivalent, C2100 (163 kN)..

Table 7. Summary of experimental results for specimens: R, C250, C2100, CD250, and CD2100

Specimen ID	R	C250	C2100	CD250	CD2100
Configuration	None	sheet	Continuous	sheet	Continuous
Layers	None	2	2	2	2
P_{cr} (kN)	15	40	40	None	None
P_u (kN)	120	153	163	132.9	156.5
Δ_u(mm)	21.34	15.55	11.93	14.2	14.5
P_{SLS}	31	55	70	None	None
k_i (kN/mm)	10.6	17.05	25	None	None
K_p(kN/mm)	1.13	3	4.6	1.6	3.5
Preloading level	None	None	None	50%	50%

Although localized repair at CD250 attained 132.9 kN, which only lost 86.8% of the capacity for the strengthened specimen C250 (153 kN), It implies that because a continuous (full-face) reinforcement configuration is more likely to effectively contain and bridge existing cracks over the entire length, it appears less sensitive to the influence of pre-existing cracking compared to the localized strengthening configuration investigated in this study

This highlights the influence of pre-damage on the post-cracking stiffness (k_p). For the 2100 series, the stiffness decreased from 4·6 kN/mm in the strengthened state (C2100) to 3·5 kN/mm in the repaired (CD2100) state. Hence the small reduction suggests the continuous FRCM layer "heals" the section by restoring a significant degree of flexural stiffness despite the 50% pre-loading damage. The 250 series, on the other hand, underwent a more drastic stiffness reduction from 3 kN/mm (C250) down to 1.6 kN/mm (CD250). These observations suggest that localized strengthening can effectively restore load-carrying capacity; however, its ability to control post-cracking deformation and stiffness degradation appears to be less pronounced compared to the continuous strengthening configuration. Counter intuitively the findings show that a full coverage repair to a damaged slab (CD2100) can give a greater ultimate capacity (156.5 kN) than localized strengthening of a healthy slab (C250 = 153 kN). This observation highlights the potential structural effectiveness of the Carbon-FRCM strengthening approach; rather than simply "repairing" an already compromised structure back to its original condition, it upgrades that structure up to a higher performance category. Overall, although zoned reinforcement (250 layout) is still the cheapest option for both applications, the continuous layout (2100) ensures better structural recovery, especially in terms of preserving normal section rigidity and crack control regarding prior major damage. It should be noted that the comparison presented in this section is limited to structural performance and relative material usage, and does not represent a comprehensive economic or cost analysis.

3.4 Influence of FRCM Coverage Ratio and Configuration

Coverage ratio of Carbon-FRCM system is crucial to finding a compromise between material saving and structural behavior. As shown in Table 7 and Fig. 3, this research focused on two principal configurations: a localized (250 series) sheet configuration that covers the high-moment region only and a continuous (2100 series) configuration that spans the entire face. Interestingly, subject to this change in the coverage area from localized patch to full surface reinforcement, the experimental data suggests only a marginal increase in ultimate load capacity; namely, C2100 was only 6.5% stronger than C250 (163 kN vs 153 kN), and CD2100 was only 17.7% superior to CD250 (156.5 kN vs 132.9 kN). Although the larger reinforcement coverage in the 2100 series provided an additional structural safety margin, this suggests the localized 250 configuration appears to provide efficient structural performance at capturing the main flexural stresses at their most crucial location, as illustrated by the load-deflection comparisons in Fig. 10.

In the control of deformations and distribution of cracks, the effect of the coverage ratio was present as the most significant factor. In Table 7, the ultimate deflection was limited to 11.93 mm for specimen C2100, which was 100% covered, and was 15.55 mm for specimen C250. This improvement in serviceability is related to the crack smearing effect identified in same full-coverage models (Fig. 7(c) and Fig. 9(c)) that the continuous mesh contributed to a more distributed tensile stress transfer across the slab tension face on the entire tension face of the slab. On the contrary, due to the unified FRCM patch boundaries, the 250 series showed almost localized cracking propagation, between the crack bands (Fig. 7; Fig. 9(b)), that could also be justified in terms of very low post cracking stiffness (k_p) values, equal to 3 kN/mm and 1.6 kN/mm for the C and CD series, respectively, compared to the higher stiffness kept by the 2100 series.

Ultimately, the choice of coverage ratio reflects a balance between structural performance and material usage. Although the 2100 configurations provide improved overall stiffness and more uniform crack control, the localized 250 configuration demonstrates effective strengthening and repair performance with reduced material usage. This trend is clearly illustrated in the integrated performance curves shown in Fig. 6. From a practical perspective, localized FRCM application can be considered an efficient approach for structural restoration, as it enables recovery of slab capacity beyond its pre-damage level while limiting the amount of reinforcement applied to critical regions. It should be noted that the experimental program was designed to provide a focused comparative assessment of strengthening configurations rather than a statistical evaluation of material variability.

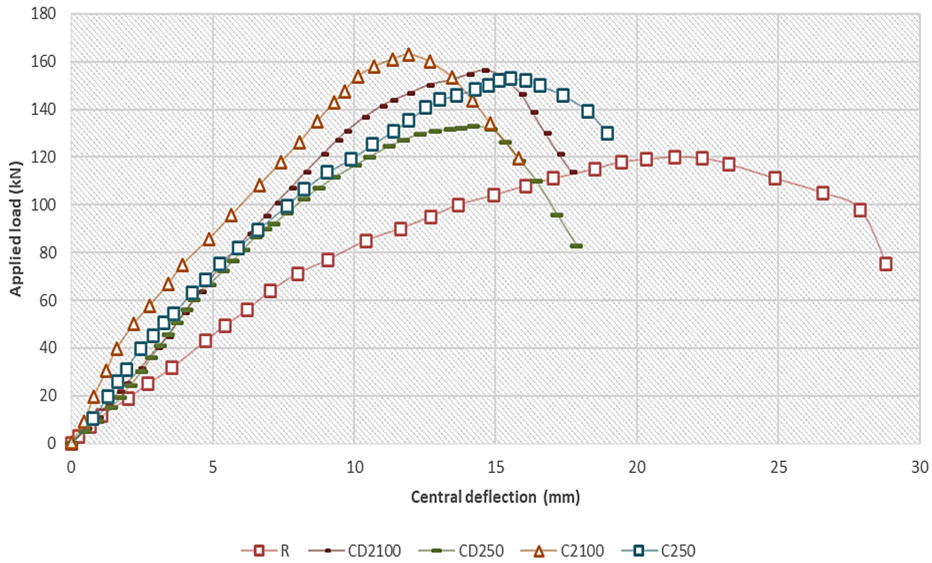

Fig. 10. Load-deflection response of specimens: R, CD2100, CD250, C2100, and C250

Although the number of specimens tested was limited, the observed behavioral trends in terms of stiffness evolution, cracking sequence, and load-carrying capacity showed consistent responses among the investigated strengthening arrangements. Under controlled laboratory conditions, the experimental findings provide meaningful insight into the structural performance of Carbon-FRCM strengthened slabs, particularly regarding the comparative behavior between localized and full-surface strengthening configurations. Nonetheless, the present study has a scope for further research with a greater number of specimens and loading conditions, which could possibly enhance the transferability of the results and a wider generalization for design-oriented purposes.

4. Conclusion

The following conclusions are drawn from the experimental results and comparative effectiveness of the Carbon-FRCM system for strengthening and repair of RC slabs:

- The Carbon-FRCM system was found to be effective within the scope of the experimental program in enhancing the structural performance of both intact and pre-damaged slabs. The increase in ultimate load capacity (P_u) of the strengthening specimens (C series) reached up to 35.8% for C2100 compared to the control slab.
- The experimental results indicate that the Carbon-FRCM system was capable of restoring and enhancing the load-carrying capacity of slabs (CD series) that were pre-loaded to 50% of the original strength. Specimen CD2100 reached 96% of the maximum capacity of its strengthened counterpart (C2100) and exceeded the original capacity of the control slab by 30.4%.
- FRCM resulted in noticeable increases in the initial stiffness (k_i) and service loads (P_{SLS}). In the first load stage, the initial stiffness of specimen C2100 was the highest at 25 kN/mm, which represents a 135.8% increase compared to the control slab (R), while C250 increased the service load to 55 kN [31 kN for reference specimen].
- The results suggest that localized strengthening (250 series) can provide effective structural improvement with reduced material usage compared to full-area coverage (2100 series) under the investigated conditions. Although a larger strengthening area was used in specimen C2100, only a 6.5% increase in ultimate load capacity was achieved compared to that of C250.
- Flexural cracks in the control slab were relatively wide, accompanied by early stiffness degradation, indicating a more brittle failure mode. In contrast, the specimens strengthened with Carbon-FRCM exhibited a more distributed cracking pattern ("crack smearing"), reflecting improved crack control and higher deformation capacity. The most uniform crack distribution and the greatest reduction in deflection were observed for the full-surface

coverage (2100 series), with a final deflection approximately 44% lower than that of the reference slab.
- No visible debonding or delamination of the FRCM layer from the concrete substrate was observed in the tested specimens. The dominant failure mode was rupture of the carbon textile, suggesting that bond transfer between the cementitious matrix and the concrete surface was effective under the applied loading conditions.

It should be noted that the conclusions presented are based on a limited experimental program and are intended to reflect observed behavior under controlled laboratory conditions rather than generalized structural performance.

5. Limitations and Future Work

This work represents an experimental study on the structural performance of Carbon-FRCM for strengthening and repair of reinforced concrete slabs. In addition, the experimental program was conducted using a limited number of specimens without repeated tests for each strengthening configuration; therefore, broader statistical validation of the observed structural trends requires further experimental investigation. The experimental program was carried out under monotonic loading, and a single pre-damage level corresponding to 50% of the ultimate capacity of the control specimen. This value represents moderate damage under controlled parameters; other damage levels or other deterioration mechanisms may affect structural response differently. Moreover, the tests were conducted in a laboratory environment and the long-term response of FRCM–concrete interface to cyclic loading or environmental effects calls for more studies.

Future research might aim to determine more optimal strengthening layouts to ensure a better efficiency of the structure with respect to the consumption of material, explore alternative types of textiles and subject the models to different loading conditions. Also, numerical modeling techniques such as finite element analysis (FEA) may be beneficial in providing a better understanding of the interfacial stress transfer mechanisms and predicting potential failure modes within FRCM-strengthened structural members.

References

[1] Kadhim EM, Altaie MR. Factors Affecting Maintenance Practises in Iraq's Hospital Buildings. Jordan Journal of Civil Engineering. 2023;17(3). https://doi.org/10.14525/JJCE.v17i3.04
[2] Harith IK, et al. Prediction of high-performance concrete strength using machine learning with hierarchical regression. Multiscale and Multidisciplinary Modeling, Experiments and Design. 2024;7(5):4911-4922. https://doi.org/10.1007/s41939-024-00467-7
[3] Abbas MK, Hamzah MK. Numerical investigation on flexural performance of hybrid concrete T-beams. In: AIP Conference Proceedings. AIP Publishing LLC; 2023. https://doi.org/10.1063/5.0166265
[4] Fan L, Shi X. Techniques of corrosion monitoring of steel rebar in reinforced concrete structures: A review. Structural Health Monitoring. 2022;21(4):1879-1905. https://doi.org/10.1177/14759217211030911
[5] Luccioni B, et al. Experimental and numerical analysis of blast response of High Strength Fiber Reinforced Concrete slabs. Engineering Structures. 2018;175:113-122. https://doi.org/10.1016/j.engstruct.2018.08.016
[6] Darwin D, Dolan CW, Nilson AH. Design of concrete structures. Vol. 2. New York, NY, USA: McGraw-Hill Education; 2016.
[7] Farahzadi L, Askarifarsangi A, Kioumarsi M. Sustainable Construction Practices in Repair and Strengthening of Concrete Bridges. In: International Conference on Concrete Repair, Rehabilitation and Retrofitting. Springer; 2024. https://doi.org/10.1007/978-3-031-75507-1_32
[8] Alam MA, Al-Amin M. Anchors for shear strengthening of damaged RC beam using bonded steel plate. Res. Eng. Struct. Mater., 2023; 9(4): 1361-1377. http://dx.doi.org/10.17515/resm2023.678st0130
[9] Hamzah MK, Rashid RSM, Hejazi F. Cyclic performance of exterior RC beam-column strengthened with different thicknesses of CFRP sheets. In: IOP Conference Series: Earth and Environmental Science. IOP Publishing; 2022. https://doi.org/10.1088/1755-1315/961/1/012069
[10] Hamzah MK. Replacement of Flexural and Shear Reinforcement of Double-Column Bridge Bent with CFRP under Combined loadings. In: IOP Conference Series: Earth and Environmental Science. IOP Publishing; 2022. https://doi.org/10.1088/1755-1315/961/1/012070

[11] Varma DA, et al. Performance Comparison of Fiber Reinforced Polymer (FRP) systems and Textile Reinforced Mortar (TRM) for Concrete Confinement at Elevated Temperature. Composites Part C: Open Access. 2025:100628. https://doi.org/10.1016/j.jcomc.2025.100628
[12] Al-Khafaji ZS, et al. Strengthening of Reinforced Concrete Slabs: A Review. In: Proceedings of the 6th International Conference on Rehabilitation and Maintenance in Civil Engineering (ICRMCE 2024). Cham, Switzerland: Springer Nature; 2024.
[13] Olivito RS, Codispoti R, Scuro C. Experimental analysis on adhesion of NFRCM Systems applied to masonry structures. In: AIMETA 2017 - Proceedings of the 23rd Conference of the Italian Association of Theoretical and Applied Mechanics. Centro Servizi d'Ateneo Srl; 2017.
[14] Sagare SS, Kirthiga R, Elavenil S. A state of art of review on strengthening of concrete structures using fabric reinforced cementitious matrix. Res Eng Struct Mater. 2024;10:1231-1260. https://doi.org/10.17515/resm2024.133ma1226rv
[15] Agossou OG, Homoro O, Amziane S. A review of the applications of natural FRCM composites. Journal of Composite Materials. 2025;59(15):1881-1915. https://doi.org/10.1177/00219983251318829
[16] Ascione F, et al. Bond-slip models for the interface between steel fabric reinforced cementitious matrix and concrete substrate. Composites Part C: Open Access. 2020;3:100078. https://doi.org/10.1016/j.jcomc.2020.100078
[17] Wang F, et al. Experimental research on bond behaviour of fabric reinforced cementitious matrix composites for retrofitting masonry walls. International Journal of Concrete Structures and Materials. 2021;15(1):22. https://doi.org/10.1186/s40069-021-00460-1
[18] Bilotta A, Lignola GP. Effects of defects on bond behavior of fiber reinforced cementitious matrix materials. Materials. 2020;13(1):164. https://doi.org/10.3390/ma13010164
[19] Al-Lami K, D'Antino T, Colombi P. Durability of fabric-reinforced cementitious matrix (FRCM) composites: A review. Applied Sciences. 2020;10(5):1714. https://doi.org/10.3390/app10051714
[20] Del Vecchio C, Di Ludovico M, Prota A. Cost and effectiveness of fiber-reinforced polymer solutions for the large-scale mitigation of seismic risk in reinforced concrete buildings. Polymers. 2021;13(17):2962. https://doi.org/10.3390/polym13172962
[21] Ombres LV, Stefano. Textile-Reinforced Mortar (TRM) as a Cementitious Composite for Structural Strengthening and Repair. AIMS Materials Science. 2025;12(3):423-452. https://doi.org/10.3934/matersci.2025022
[22] Qin LZ, Yi YD, Fang H. Experimental Study on Flexural Capacity of Corroded RC Slabs Reinforced with Basalt Fiber Textile. Applied Sciences. 2021;11(1):144. https://doi.org/10.3390/app11010144
[23] Calabrese AS, et al. Long-term behavior of PBO FRCM and comparison with other inorganic-matrix composites. Materials. 2022;15(9):3281. https://doi.org/10.3390/ma15093281
[24] Napoli A, Realfonzo R. Compressive strength of concrete confined with fabric reinforced cementitious matrix (FRCM): Analytical models. Composites Part C: Open Access. 2020;2:100032. https://doi.org/10.1016/j.jcomc.2020.100032
[25] Sika AG. Sika MonoTop®-612: Product Data Sheet. Switzerland: Sika AG; 2023.
[26] European Committee for Standardization (CEN). EN 1504-3:2005 - Products and systems for the protection and repair of concrete structures - Definitions, requirements, quality control and evaluation of conformity - Part 3: Structural and non-structural repair. European Committee for Standardization (CEN); 2005.
[27] Tetta ZC, Koutas LN, Bournas DA. Textile-reinforced mortar (TRM) versus fiber-reinforced polymers (FRP) in shear strengthening of concrete beams. Composites Part B: Engineering. 2015;77:338-348. https://doi.org/10.1016/j.compositesb.2015.03.055
[28] Wu C, Pan Y, Yan L. Mechanical properties and durability of textile reinforced concrete (TRC)-a review. Polymers. 2023;15(18):3826. https://doi.org/10.3390/polym15183826
[29] Chahar AS, Pal P. Study on various properties of reinforced concrete-A review. Materials Today: Proceedings. 2022;65:597-602. https://doi.org/10.1016/j.matpr.2022.03.193
[30] Standard TO. Standard Specification for Deformed and Plain Carbon Steel Bars for Concrete. 2004.
[31] Golewski GL. Mechanical properties and brittleness of concrete made by combined fly ash, silica fume and nanosilica with ordinary Portland cement. AIMS Materials Science. 2023;10(3). https://doi.org/10.3934/matersci.2023021
[32] British Standards Institution (BSI). BS 1881-116:1983 - Testing concrete: Method for determination of compressive strength of concrete cubes. London, UK: BSI; 1983.
[33] British Standards Institution (BSI). BS 1881-117:1983 - Testing concrete: Method for determination of tensile splitting strength. London, UK: BSI; 1983.
[34] British Standards Institution (BSI). BS 1881-118:1983 - Testing concrete: Method for determination of flexural strength. London, UK: BSI; 1983.
[35] Kadhim MM, et al. Analysis and design of two-way slabs strengthened in flexure with FRCM. Engineering Structures. 2022;256:113983. https://doi.org/10.1016/j.engstruct.2022.113983